

Electrophysiological properties of maxillary trigeminal A β -afferent neurons of rats

Yuya Okutsu, Akihiro Yamada, Sotatsu Tonomura, Ryan J Vaden, and Jianguo G Gu 

Molecular Pain
Volume 17: 1–13
© The Author(s) 2021
Article reuse guidelines:
sagepub.com/journals-permissions
DOI: 10.1177/17448069211021271
journals.sagepub.com/home/mpx



Abstract

A β -afferents in maxillary or V2 trigeminal ganglion (TG) neurons are somatosensory neurons that may be involved in both non-nociceptive and nociceptive functions in orofacial regions. However, electrophysiological properties of these V2 trigeminal A β -afferent neurons have not been well characterized so far. Here, we used rat *ex vivo* trigeminal nerve preparations and applied patch-clamp recordings to large-sized V2 TG neurons to characterize their electrophysiological properties. All the cells recorded had afferent conduction velocities in the range of A β -afferent conduction speeds. However, these V2 trigeminal A β -afferent neurons displayed different action potential (AP) properties. APs showed fast kinetics in some cells but slow kinetics with shoulders in repolarization phases in other cells. Based on the derivatives of voltages in AP repolarization with time (dV/dt), we classified V2 trigeminal A β -afferent neurons into four types: type I, type II, type IIIa and type IIIb. Type I V2 trigeminal A β -afferent neurons had the largest dV/dt of repolarization, the fastest AP conduction velocities, the shortest AP and afterhyperpolarization (AHP) durations, and the highest AP success rates. In contrast, type IIIb V2 trigeminal A β -afferent neurons had the smallest dV/dt of AP repolarization, the slowest AP conduction velocities, the longest AP and AHP durations, and the lowest AP success rates. The type IIIb cells also had significantly lower voltage-activated K⁺ currents. For type II and type IIIa V2 trigeminal A β -afferent neurons, AP parameters were in the range between those of type I and type IIIb V2 trigeminal A β -afferent neurons. Our electrophysiological classification of V2 trigeminal A β -afferent neurons may be useful in future to study their non-nociceptive and nociceptive functions in orofacial regions.

Keywords

Trigeminal, A β -afferent, pain, action potentials, orofacial, patch-clamp

Date Received: 24 March 2021; Revised 14 April 2021; accepted: 8 May 2021

Introduction

Primary afferent nerves are commonly classified into C-, A δ - and A α / β -afferents (cutaneous afferents) or into group IV, III, II and I fibers (muscle afferents) on the basis of their conduction velocities.¹ The somas of primary afferents, located in the dorsal root ganglions (DRGs) and trigeminal ganglions (TGs), largely vary in size, and are correlated with afferent types. Generally, small- to medium-sized afferent neurons give rise to non-myelinated C-fibers or thinly myelinated A δ -fibers (or IV- and III-fibers of muscle afferents), whereas large-sized DRG and TG neurons give rise to well myelinated A β /A α - fibers (or II and I-fibers of muscle afferents).² Electrophysiological properties and functions of small-sized afferent neurons have been extensively studied. The afferent fibers of most

small-sized DRG and TG neurons are believed to be involved in nociception induced by high-intensity mechanical, thermal, and chemical stimulation.² In contrast, it is generally thought that A β -primary afferents are non-nociceptors, mainly comprising low threshold mechanoreceptors (LTMRs) although some LTMRs are A δ - and C-afferents.³ However, studies have shown in different species that many A β -primary afferents of

Department of Anesthesiology and Perioperative Medicine, University of Alabama at Birmingham, Birmingham, AL, USA

Corresponding Author:

Jianguo G Gu, Department of Anesthesiology and Perioperative Medicine, University of Alabama at Birmingham, 901 19TH Street South, BMR II 210, Birmingham, AL 35294, USA.

Email: jianguogu@uabmc.edu



the DRGs can encode high threshold mechanical and thermal stimuli to function in nociception.^{4,5} The DRG neurons of these afferents are termed nociceptive A β -afferent neurons.⁴ For example, in a previous study in cats, it has been shown that although most A β -afferents could be activated by gentle mechanical stimulation, a small subset with conduction velocities in the low end of the A β afferent range encode nociceptive stimuli.⁶

Nociceptive A β -afferents from DRGs have been suggested to be first responders to noxious stimuli and play an essential role in pain under physiological conditions.^{4,5,7} Many nociceptive A β -afferents from DRGs are high threshold mechanoreceptors (HTMRs).^{4,7} It has been hypothesized that under pathological conditions the mechanical threshold of these A β -afferent HTMRs may be reduced, leading to mechanical hyperalgesia/allodynia.⁸ On the other hand, non-nociceptive A β -afferents from DRGs are mainly LTMRs involved in tactile sensations.³ Non-nociceptive A β -afferents may also be involved in mechanical allodynia under pathological conditions when central sensitization occurs in the spinal cord dorsal horn.⁹ Thus far, the contribution of A β -afferents in sensory disorders involving pathological pain have been poorly studied, partially because limited attempts have been made to differentiate between non-nociceptive and nociceptive A β -afferents.

Using intracellular recordings made from DRG neurons in anesthetized animals, previous studies have characterized electrophysiological properties of both non-nociceptive A β -afferents and nociceptive A β -afferents.^{4,10} Neurons in somatosensory ganglia have been known to be heterogeneous not only in cell size, but also in electrophysiological properties and sensory functions. For example, broad AP spikes with shoulders were commonly found in DRG and TG neurons with unmyelinated C-afferent nociceptors.^{5,11} Similarly, in DRGs, it has been demonstrated that nociceptive afferents in either A δ - or A β -afferent conduction velocity range also exhibit broad AP spikes with shoulders.⁴ In DRGs, nociceptive A β -afferents differed from non-nociceptive A β -afferents in that the former had greater AP duration, longer AHP duration, and prominent shoulder on their repolarization.^{6,11} These electrophysiological properties are helpful for classifying non-nociceptive-like and nociceptive-like A β -afferents of DRG neurons.

Orofacial regions are innervated by maxillary branches (V2 branches) of trigeminal nerves, which can undergo hyper-excitability leading to thermal and mechanical allodynia under pathological conditions.^{12,13} V2 trigeminal nerves only contain sensory nerve fibers but proprioceptive A α -afferent fibers are not present in V2 trigeminal nerves. Previous electrophysiological studies have mainly focused on small-sized nociceptive-like TG neurons including V2 trigeminal afferent neurons that innervate orofacial regions.^{12,14,15} Yet electrophysiological

properties of A β -afferent neurons in TGs have not been well characterized so far. In the present study we characterized electrophysiological properties of V2 trigeminal A β -afferent neurons by using *ex vivo* rat trigeminal nerve preparations and patch-clamp recording technique, and found these neurons can be classified into at least 4 subtypes.

Materials and methods

Animals

Sprague-Dawley rats of both males and females aged at 11–15 weeks were used. Animal care and use conformed to NIH guidelines for care and use of experimental animals. Experimental protocols were approved by the Institutional Animal Care and Use Committee (IACUC) of the University of Alabama at Birmingham.

Patch-clamp recordings from large V2 trigeminal afferent neurons in *ex vivo* whole-mount trigeminal ganglion preparations

Trigeminal ganglions (TGs) with attached infraorbital nerve bundles (~15 mm) were rapidly dissected out and placed in an ice cold Krebs solution (see below). Connective tissues on the surface of the TGs were carefully removed with a fine forceps. TGs with their infraorbital nerve bundles were then affixed in a recording chamber by a tissue anchor and submerged in a Krebs solution that contained (in mM): 117 NaCl, 3.5 KCl, 2.5 CaCl₂, 1.2 MgCl₂, 1.2 NaH₂PO₄, 25 NaHCO₃, and 11 glucose. The Krebs solution was saturated with 95% O₂ and 5% CO₂, had pH of 7.35, and osmolarity of 324 mOsm, and maintained at room temperature of 24 °C. TGs were exposed to 0.05% dispase II and 0.05% collagenase in the Krebs solution for 5 min, then continuously perfused at 2 ml/min with the Krebs solution. Under an infrared-differential interference contrast (IR-DIC microscope), whole-cell patch-clamp recordings were performed on V2 TG neurons ranging 40–55 μ m in diameter. Recording electrode internal solution contained (in mM): 105 K-gluconate, 35 KCl, 0.5 CaCl₂, 2.4 MgCl₂, 5 EGTA, 10 HEPES, 5 Na₂ATP and 0.33 GTP-TRIS salt; the pH of the solution was adjusted to 7.35 with KOH. The electrode resistance ranged from 4 to 6 M Ω . The junction potential of the recording condition was 12 mV as calculated based on ionic concentrations of internal and the Krebs bath solutions by using the pCLAMP 10 software (Molecular Devices). After establishing whole-cell access, recordings were first performed under the conventional current-clamp configuration. Action potentials (APs), recorded at the soma of large-sized V2 TG neurons, were evoked at the peripheral end of trigeminal V2 branches (the infraorbital nerves) using a

suction stimulation electrode. The suction stimulation electrode was fire-polished with tip size of ~ 1 mm in diameter. The peripheral end of the infraorbital nerve was aspirated into the suction stimulation electrode by a negative pressure. APs were evoked by monophasic square wave pulses generated by an electronic stimulator (Master-8) and delivered via a stimulation isolator and the suction stimulation electrode to the peripheral ends of the infraorbital nerves. The duration of the stimulation pulse was 200 μ s each pulse. The stimulation intensity was twofold the threshold intensity (30 μ A or higher) for eliciting APs from these afferent nerves. APs evoked by the peripheral nerve stimulations were used for determining AP parameters including derivatives of repolarization with time (dV/dt), amplitude, half-width, and afterhyperpolarization duration (AHP). In one set of experiments, APs were elicited by the electrical stimuli at the frequencies of 1, 10, 20, 50, 100, 200, 500, and 1000 Hz. This set of experiments allowed measurement of AP success rate in response to stimuli at different stimulation frequencies.

APs were also recorded by directly injecting depolarizing current into V2 trigeminal A β -afferent neurons. This was done under the current-clamp configuration with step currents injected from recording electrodes into the somas of V2 trigeminal A β -afferent neurons. The current steps were from -200 pA to 4000 pA with increments of 200 pA per step and the duration of each step was 1 s. APs evoked by current steps were used to determine membrane input resistance, and AP parameters including dV/dt of repolarizations, rheobase, amplitude, half width, and AP thresholds.

Recordings were also performed under the voltage-clamp configuration with neurons held at -72 mV (voltage command of -60 mV). Voltage steps were applied from -102 mV to $+58$ mV (voltage command of -90 to $+70$ mV) with increments of 10 mV each step and a step duration of 500 ms. Unless otherwise indicated, membrane voltages mentioned in the texts for this set of experiments have been corrected for the calculated junction potentials of 12 mV.

Signals of current-clamp and voltage-clamp experiments were amplified using a MultiClamp 700B amplifier (Molecular Device). Signals of current-clamp recordings were low-pass filtered at 2 kHz and sampled at 50 kHz. The sampling at high frequency of 50 kHz is necessary for a high resolution measurement of AP parameters. Signals of voltage-clamp recordings were low-pass filtered at 2 kHz and sampled at 10 kHz. The signals were sampled using the pCLAMP 11 software (Molecular Devices).

Data analysis

In the present study TGs were obtained from 6 male and 21 female rats, and the data from both sexes were pooled

together as we did not observe any sex differences in the AP properties of V2 trigeminal A β -afferent neurons. Conduction velocity was calculated based on the latency of APs and the length of axons. The latency of an AP was measured from the time of stimulation that was marked by a stimulation artifact to the time when the AP was initiated at the recorded TG neuron. The length of the axon was the distance between the stimulation site and the recording site. Input resistance was measured with a -10 mV voltage step from the membrane holding voltage of -72 mV. AP amplitude was measured from AP peak to AP afterhyperpolarization. AP half width was measured as the duration from 50% of AP upstroke to 50% of AP repolarization. AHP duration was measured as the duration between AHP peak and the potential of 80% AHP recovery (i.e. AHP80%). Membrane and AP parameters as well as voltage-activated currents were analyzed using Clampfit 11 software. Unless otherwise indicated, all data are reported as mean \pm SEM of n independent observations. Statistical comparisons were made using GraphPad Prism 8 software with * $p < 0.05$, ** $p < 0.01$, and *** $p < 0.001$, Student's t -test or one-way ANOVA with Tukey's post-hoc tests for multiple groups.

Results

The maxillary nerves or V2 branches of the trigeminal nerves are somatosensory nerves that innervate orofacial regions (Figure 1(a)). The somas of these trigeminal afferent nerves are located in the V2 part in the trigeminal ganglion¹² (Figure 1(b)). Under an IR-DIC microscope, individual TG neurons in our *ex vivo* TG preparations could be visualized in the V2 TG regions, and these V2 TG neurons showed different cell sizes (Figure 1(b) and (c)). Since in the present study we focused on A β -afferent neurons that innervate orofacial regions, we applied patch-clamp recordings to large V2 TG neurons in our *ex vivo* TG preparations (Figure 1(c) and (d)). The V2 TG neurons selected for our patch-clamp recordings had mean diameters ranging from 40 to 55 μ m ($n = 51$). Of these cells, 42 of them (82%) had mean diameters ≥ 45 μ m and 9 of them had mean diameters ≥ 40 but smaller than 45 μ m. Overall, the averaged mean diameters of the recorded V2 TG neurons were 46.0 ± 0.37 μ m ($n = 51$).

To determine if these cells were A β -afferent neurons, action potentials (AP) were recorded under the current-clamp configuration from the somas of large-sized V2 TG neurons while electrical stimuli were applied to the peripheral sites of infraorbital nerve bundles (ION, Figure 1(b) and (e)). This allowed us to determine the conduction velocities of these afferents. In each of the V2 TG neurons recorded in the present study, APs appeared after short latencies following the peripheral electrical

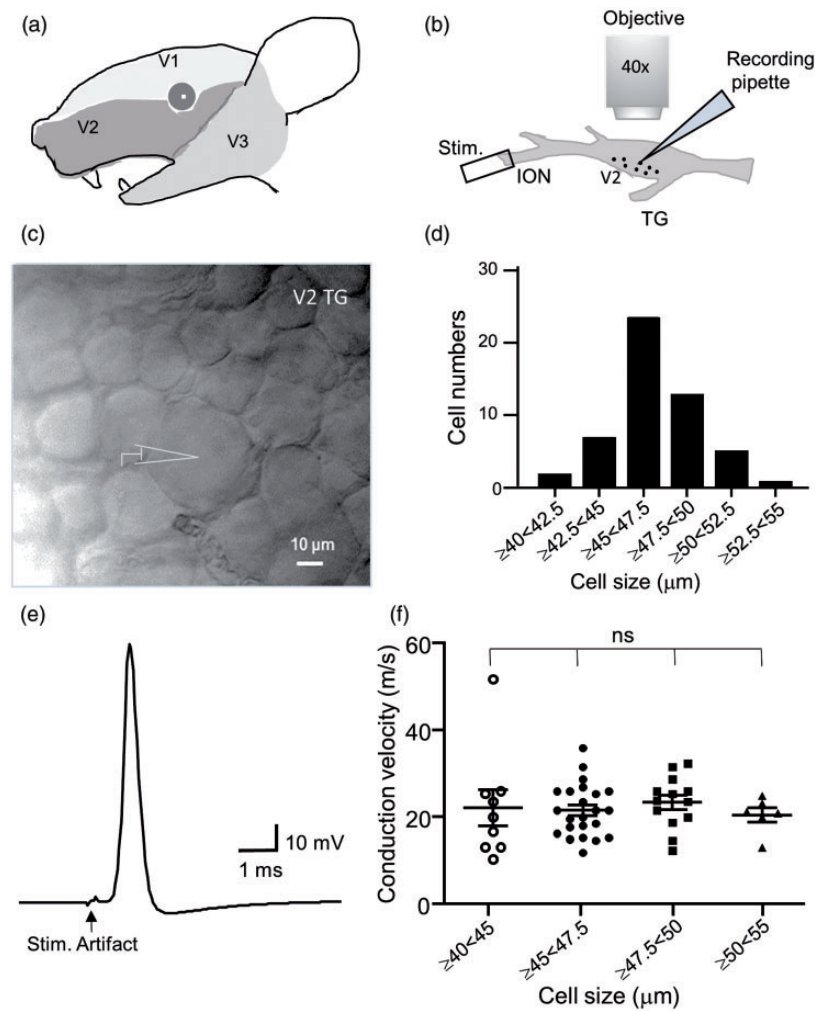


Figure 1. Large-sized V2 TG neurons and their conduction velocities determined by patch-clamp recordings with *ex vivo* trigeminal nerve preparations. (a) Illustration of orofacial regions where the V2 branches of trigeminal nerves innervate. (b) Diagram illustrates electrophysiology recording setup. *Ex vivo* trigeminal nerve preparations with V2 afferent nerve bundle (infraorbital nerves) were used and illustrated in the diagram. Patch-clamp recordings were performed from large-sized neurons in the V2 region of each TG ganglion. A suction stimulation electrode was used to elicit action potentials (APs) by stimulating the infraorbital nerves (ION), the V2 branch of trigeminal nerves. (c) Image shows V2 TG neurons in an *ex vivo* TG preparation as viewed under a 40X objective. Note that a large-sized TG neuron is located at the center of the field, and recordings were applied to this type of large TG neurons in the present study. (d) Histogram of cell size distribution for the V2 TG neurons recorded in the present studies. (e) Sample trace shows an action potential recorded from a large-sized V2 TG neuron following electrical stimulation applied to ION. Arrow indicates stimulation artifact, which allowed to determine the conduction velocity of the afferent being recorded. (f) Comparison of the conduction velocities of afferent fibers with different soma size groups of ≥ 40 and < 45 μm ($n = 9$), ≥ 45 and < 47.5 μm ($n = 23$), ≥ 47.5 and < 50 μm ($n = 13$), and ≥ 50 and < 55 μm ($n = 6$). In f, each symbol represents an individual experimental observation, mean \pm SEM values are also shown; ns, no significant difference.

stimulation (Figure 1(e)). The conduction velocities of APs were 22.2 ± 4.2 m/s for the V2 TG neurons with mean diameters ≥ 40 and < 45 μm ($n = 9$), 21.7 ± 1.3 m/s for the V2 TG neurons with mean diameters ≥ 45 and < 47.5 μm ($n = 23$), 23.5 ± 1.7 m/s for the V2 TG neurons with mean diameters ≥ 47.5 and < 50 μm ($n = 13$), and 20.6 ± 1.7 m/s for the V2 TG neurons with mean diameters ≥ 50 μm ($n = 6$). There were no significant differences in the conduction velocities among the cell-size groups of these V2 TG neurons (Figure 1(f)).

The conduction velocities measured from these V2 TG neurons all fell into the range of the conduction speed of A β -afferent fibers,⁴ and we therefore regard them as V2 trigeminal A β -afferent neurons.

APs recorded from the V2 trigeminal A β -afferent neurons following electrical stimulation of the ION nerves displayed three main types based on the slopes of their repolarization phases (Figure 2(a) to (c)). This was more distinguishable with the derivatives of voltages with time (dV/dt) in the repolarization phases (Figure 2

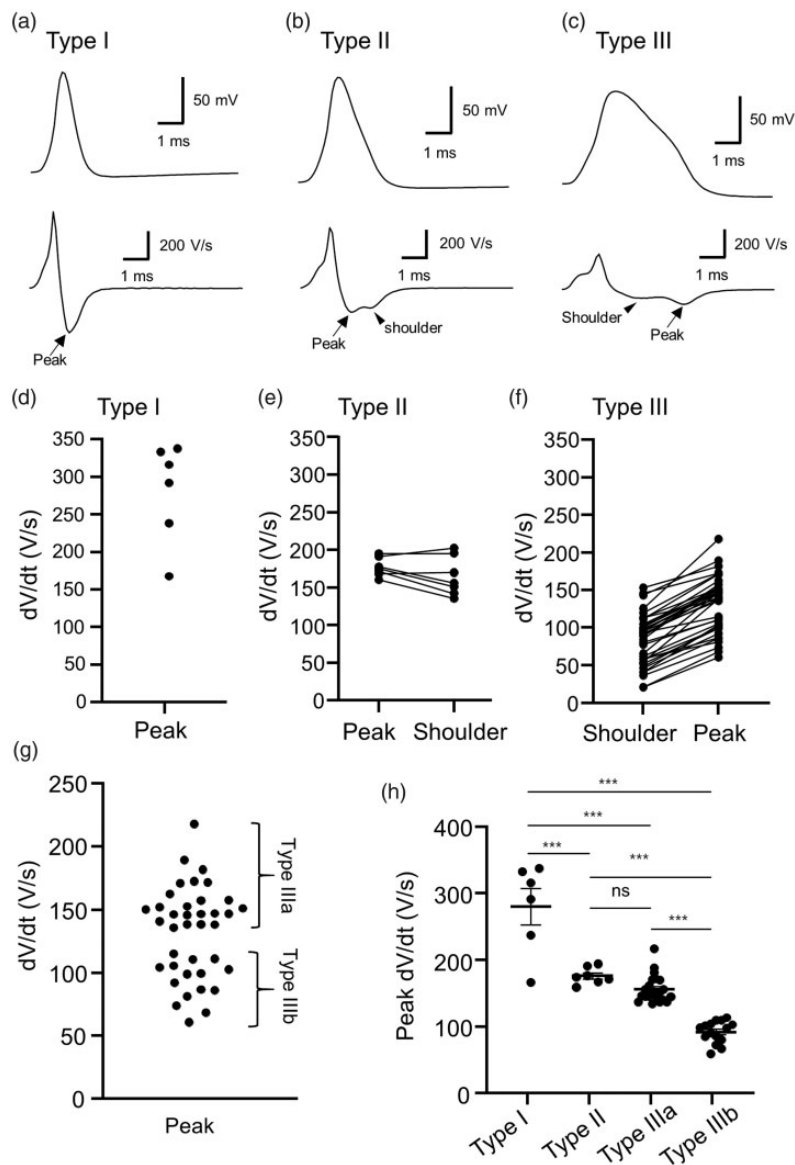


Figure 2. Classification of V2 trigeminal A β -afferent neurons based on their action potential kinetics. (a to c) Sample traces show three types of action potentials (top panels) and their derivatives with time (dV/dt, bottom panels). (d to f) Plots of the dV/dt values at the negative peaks (arrows indicated in (a) to (c)) and shoulders (arrowhead indicated in (a) to (c)) of AP repolarizations in type I (d, n = 6), type II (e, n = 7), and type III (f, n = 38) V2 trigeminal A β -afferent neurons. (g) Reclassifying type III into type IIIa (n = 23) and type IIIb (n = 15) groups based on the clusters of the negative peak dV/dt values of AP repolarization. (h) Comparisons of dV/dt values at the negative peaks of AP repolarizations among type I (n = 6), type II (n = 7), type IIIa (n = 23), and type IIIb (n = 15) V2 trigeminal A β -afferent neurons. In h, each symbol represents an individual experimental observation, mean \pm SEM values are also shown; ns, no significant difference, ***P < 0.001.

(a) to (c)). The first type (type I) showed rapid AP repolarization, and the dV/dt in the repolarization phase showed linear acceleration with a single large-sized negative peak (Figure 2(a) and (d)). The second type (type II) showed relatively slower AP repolarization and the dV/dt in the repolarization phase showed nonlinear acceleration with a medium-sized negative peak and a narrow negative shoulder (Figure 2(b) and (e)). The third type (type III) showed very slow AP

repolarization with a clear shoulder in the repolarization phase (Figure 2(c)), and the dV/dt in the repolarization phase showed slow acceleration with a broad negative shoulder followed by a small negative peak (Figure 2(b) and (f)). Examination of the negative peaks of the dV/dt in the type III APs revealed two clusters of dV/dt values (Figure 2(g)). We arbitrarily divided them into type IIIa for the APs with relatively larger dV/dt and type IIIb for APs with relatively smaller dV/dt values (Figure 2(g)).

Based on the aforementioned AP types, we attributed these neurons into type I, type II, type IIIa, and type IIIb V2 trigeminal A β -afferent neurons accordingly. We compared dV/dt values of APs of the four types of V2 trigeminal A β -afferent neurons (Figure 2(h)). As shown in Figure 2(h), the dV/dt values of the negative peaks of type I (280.0 ± 27.1 V/s, $n = 6$) were significantly higher than those of type II (177.3 ± 4.7 V/s, $n = 7$), type IIIa (157.1 ± 4.1 V/s, $n = 23$), and type IIIb (93.2 ± 4.2 V/s, $n = 15$) V2 trigeminal A β -afferent neurons. The dV/dt values of the negative peaks of type IIIb ($n = 15$) were the smallest and were significantly lower than those of type I, type II and type IIIa V2 trigeminal A β -afferent neurons.

We next characterized other properties of these four types of V2 trigeminal A β -afferent neurons. There were no significant differences in the cell sizes (Figure 3(a)) and resting membrane potentials (Figure 3(b)) among the four types of V2 trigeminal A β -afferent neurons. On the other hand, the conduction velocities of the type IIIb V2 trigeminal A β -afferents (16.0 ± 0.9 m/s, $n = 15$) were significantly slower than the other three types of V2 A β -afferents (Figure 3(c)). There were no significant differences in conduction velocities among the type I (29.7 ± 4.6 m/s, $n = 6$), type II (23.2 ± 1.8 m/s, $n = 7$) and type IIIa (23.8 ± 1.2 m/s, $n = 23$) V2 trigeminal A β -afferents. AP half widths were the shortest in type I (0.41 ± 0.05 ms, $n = 6$) and the longest in type IIIb V2 (1.76 ± 0.12 ms, $n = 15$) trigeminal A β -afferent neurons (Figure 3(d)). AP half widths were 0.62 ± 0.02 ms ($n = 7$) for type II and 0.93 ± 0.03 ms ($n = 7$) for type IIIa, and were significantly shorter than those of type IIIb V2 trigeminal A β -afferent neurons (Figure 3(d)). AP amplitudes were significantly smaller in type I in comparison with type II V2 trigeminal A β -afferent neurons, but there were no significant differences among other types of V2 trigeminal A β -afferent neurons (Figure 3(e)). AHP80% durations were shown to be the shortest in type I and the longest in type IIIb V2 A β -afferent neurons. The AHP80% durations of type IIIb V2 trigeminal A β -afferent neurons (179.0 ± 21.0 ms, $n = 15$) were significantly longer than those of type I (14.1 ± 7.1 ms, $n = 6$), type II (32.6 ± 6.7 ms, $n = 7$) and type IIIa (94.9 ± 10.2 ms, $n = 22$) V2 trigeminal A β -afferent neurons (Figure 3(f)).

We determined success rates of AP conduction along different types of V2 trigeminal A β -afferents in responses to electrical stimuli at different stimulation frequency. In this set of experiments, APs were elicited by twofold threshold stimuli at the peripheral sites of infraorbital nerves and recordings were made from the somas of the V2 trigeminal A β -afferent neurons. At low frequency stimuli of 1 and 10 Hz, APs could be reliably elicited and recorded with a 100% success rate for all four types of V2 trigeminal A β -afferents (Figure 4(a)

and (b)). At the stimulation frequency of 20 Hz, AP success rates were reduced to $32.2 \pm 11.1\%$ ($n = 8$) in type IIIb V2 trigeminal A β -afferents but no significant reduction in AP success rates occurred in other three types of V2 trigeminal A β -afferents. At the stimulation frequency of 50 Hz, AP success rates were greatly reduced to $8.1 \pm 3.8\%$ ($n = 8$) in type IIIb V2 trigeminal A β -afferents and also significantly reduced to $34.2 \pm 5.5\%$ ($n = 14$) in type IIIa V2 trigeminal A β -afferents but AP success rates were not significantly reduced in both type I and type II V2 trigeminal A β -afferents. At a high frequency of 100 Hz stimulation, AP success rates were reduced to $25.7 \pm 5.8\%$ ($n = 7$) in type II, to $7.9 \pm 2.2\%$ ($n = 24$) in type IIIa, and to $4.2 \pm 1.5\%$ ($n = 15$) in type IIIb V2 trigeminal A β -afferents, but AP success rates of type I V2 trigeminal A β -afferents remained to be high ($86.2 \pm 8.8\%$, $n = 6$). However, at the frequency of ≥ 200 Hz, AP success rates were also significantly reduced in type I V2 trigeminal A β -afferents, and almost all the 4 types of V2 trigeminal A β -afferents failed to follow the stimuli at the frequency of 1000 Hz (Figure 4(b)). Plotting the AP success rates over stimulation frequencies show sigmoid relationships (Figure 4(c)), and from these curves we determined frequency at which AP success rate or failure rate was at 50% (FS₅₀, Figure 4(c) and (d)). The FS₅₀ values were 167.8 ± 16.8 Hz ($n = 6$) for type I, 85.1 ± 4.9 Hz ($n = 7$) for type II, 48.7 ± 3.6 Hz ($n = 24$) for type IIIa, and 30 ± 6.0 Hz ($n = 15$) for type IIIb V2 trigeminal A β -afferents, respectively.

In the above experiments APs were elicited by applying electrical stimulation to the peripheral sites. We next determined AP properties when APs were elicited by directly injecting depolarizing step currents into the somas of the four types of V2 trigeminal A β -afferent neurons. The injection of depolarizing step currents resulted in membrane depolarization and AP firing once the depolarization reached AP thresholds (Figure 5(a) to (c)). The repolarization phase of APs elicited by the step current injections showed features similar to APs elicited by electrical stimulation to the peripheral sites of V2 trigeminal A β -afferents. The type I V2 trigeminal A β -afferent neurons showed rapid AP repolarization, and the dV/dt in AP repolarization phase showed linear acceleration with a large and sharp negative peak (Figure 5(a)). The type IIIb V2 trigeminal A β -afferent neurons showed slow AP repolarization, and the dV/dt in AP repolarization phase showed slow acceleration with a broad negative shoulder followed by a small negative peak (Figure 5(c)). The type II (Figure 5(b)) and type IIIa (not illustrated) V2 trigeminal A β -afferent neurons showed features between those of type I and type IIIb. Overall, the dV/dt values of the negative peaks of AP repolarization (Figure 5(d)) were 208.3 ± 22.8 V/s ($n = 6$) in type I, 120.7 ± 7.9 V/s ($n = 7$) in type II, 117.9 ± 5.9 V/s ($n = 25$) in type IIIa, and 79.8 ± 5.5 V/s

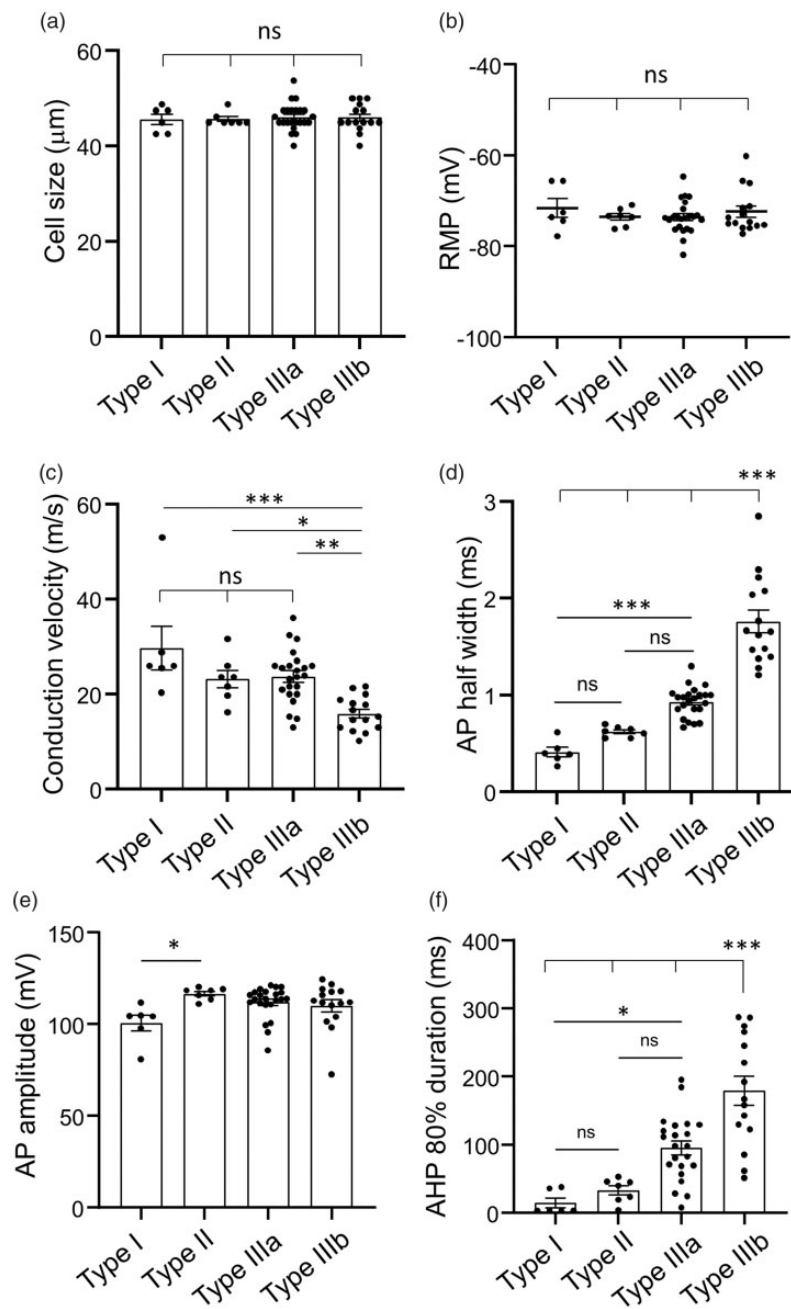


Figure 3. Electrophysiological properties of different types of V2 trigeminal A β -afferent neurons. Bar graphs show the comparisons among four types of V2 trigeminal A β -afferent neurons for their cell sizes (a), resting membrane potentials (RMP, b), conduction velocities (c), AP half widths (d), AP amplitudes (e), and AHP80% (f). Sample sizes (n) in (a) to (f) are type I = 6, type II = 7, type IIIa = 23, and type IIIb = 15. Each symbol represents an individual experimental observation, mean \pm SEM values are also shown; ns, no significant difference, * P < 0.05, ** P < 0.01, *** P < 0.001.

(n = 15) in type IIIb V2 trigeminal A β -afferent neurons. AP half widths were the shortest in type I (0.44 ± 0.04 ms, n = 6) and longest in type IIIb (2.24 ± 0.30 ms, n = 11) V2 trigeminal A β -afferent neurons. AP half widths were 0.72 ± 0.03 ms (n = 7) in type II and 1.35 ± 0.09 ms (n = 18) in type IIIa V2 trigeminal A β -afferent neurons, and were significantly shorter than

those of type IIIb V2 trigeminal A β -afferent neurons (Figure 5(e)). AP thresholds were -39.3 ± 1.45 mV (n = 6), -44.6 ± 1.48 mV (n = 7), -40.2 ± 2.4 mV (n = 18) and -43.4 ± 0.8 mV (n = 11) in type I, type II, type IIIa, and type IIIb V2 trigeminal A β -afferent neurons, respectively, and were not significantly different among these V2 trigeminal A β -afferent neurons

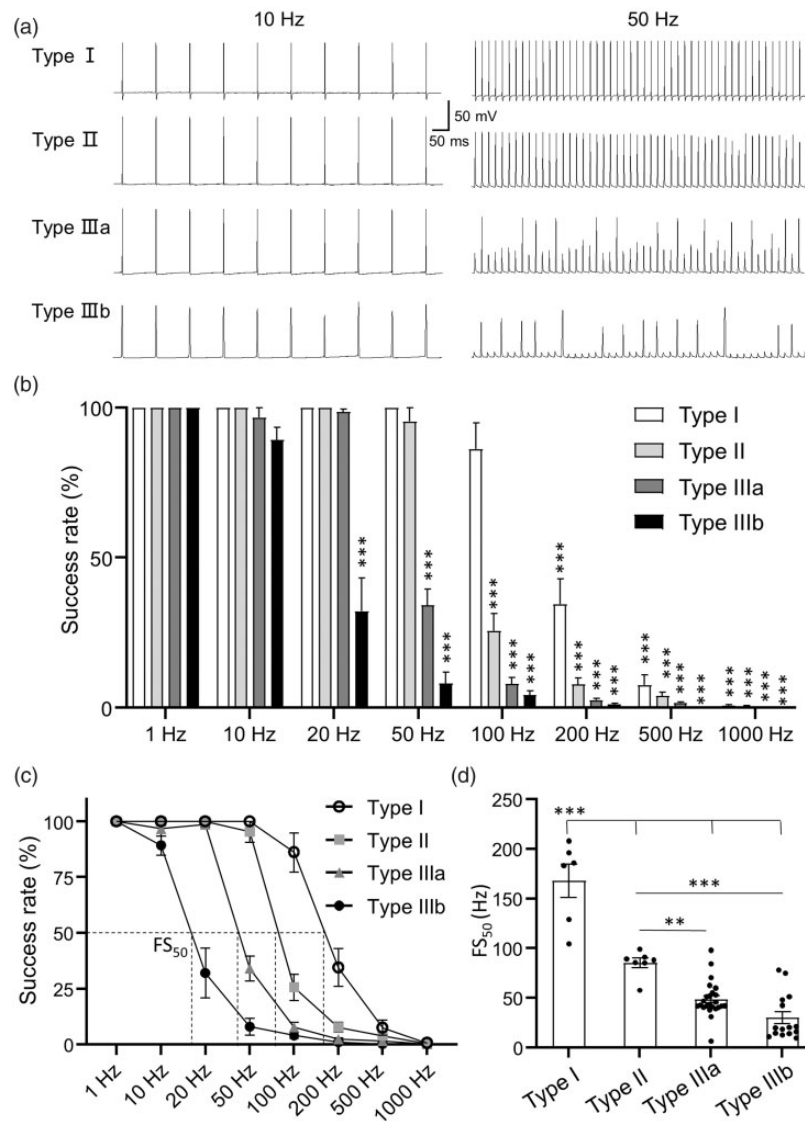


Figure 4. Success rates of action potential conduction in different types of V2 trigeminal A β -afferents. (a) Sample traces show APs recorded from the somas of four different types of V2 trigeminal A β -afferent neurons following the electrical stimulation at the peripheral sites of infraorbital nerves. The stimulation was applied at 10 Hz (left panels) and 50 Hz (right panels). From top to bottom, type I (first set), type II (second set), type IIIa (third set), and type IIIb (fourth set). A reduction of AP success rates can be seen at 50 Hz in type IIIa and type IIIb V2 trigeminal A β -afferents. (b) Bar graphs show AP success rates at different stimulation frequency in type I ($n = 6$, open bars), type II ($n = 7$, light gray bars), type IIIa ($n = 23$, darker gray bars), and type IIIb ($n = 15$, black bars) V2 trigeminal A β -afferents. Comparisons were made with the success rates at 1 Hz in each type. (c) Plots of AP success rate at different stimulation frequency for type I (open circles, $n = 6$), type II (gray squares, $n = 7$), type IIIa (gray triangles, $n = 23$), and type IIIb (solid circles, $n = 15$) V2 trigeminal A β -afferents. Dashed lines indicate stimulation frequency at which 50% success rates remain (FS₅₀) for each type of V2 trigeminal A β -afferents. (d) Summary data of FS₅₀ values of type I (1st bar, $n = 6$), type II (2nd bar, $n = 7$), type IIIa (3rd bar, $n = 23$), and type IIIb (4th bar, $n = 15$) V2 trigeminal A β -afferents. Data represent mean \pm SEM; ** $P < 0.01$, *** $P < 0.001$.

(Figure 5(f)). AP amplitudes were shown no significant differences among these V2 trigeminal A β -afferent neurons (Figure 5(g)). AP rheobases were relatively lower in type I and type IIIb V2 trigeminal A β -afferent neurons in comparison with type IIIa V2 trigeminal A β -afferent neurons (Figure 5(h)). There were no significant differences in input resistances of the four different types of V2 trigeminal A β -afferent neurons (Figure 5(i)).

Under the voltage-clamp configurations, we examined membrane currents evoked by depolarizing voltage steps in V2 trigeminal A β -afferent neurons. For all the four types of V2 trigeminal A β -afferent neurons, depolarizing voltage steps evoked transient inward currents at initial stage which were followed by large outward currents (Figure 6(a)). The transient inward currents were voltage-activated Na⁺ currents and the outward currents

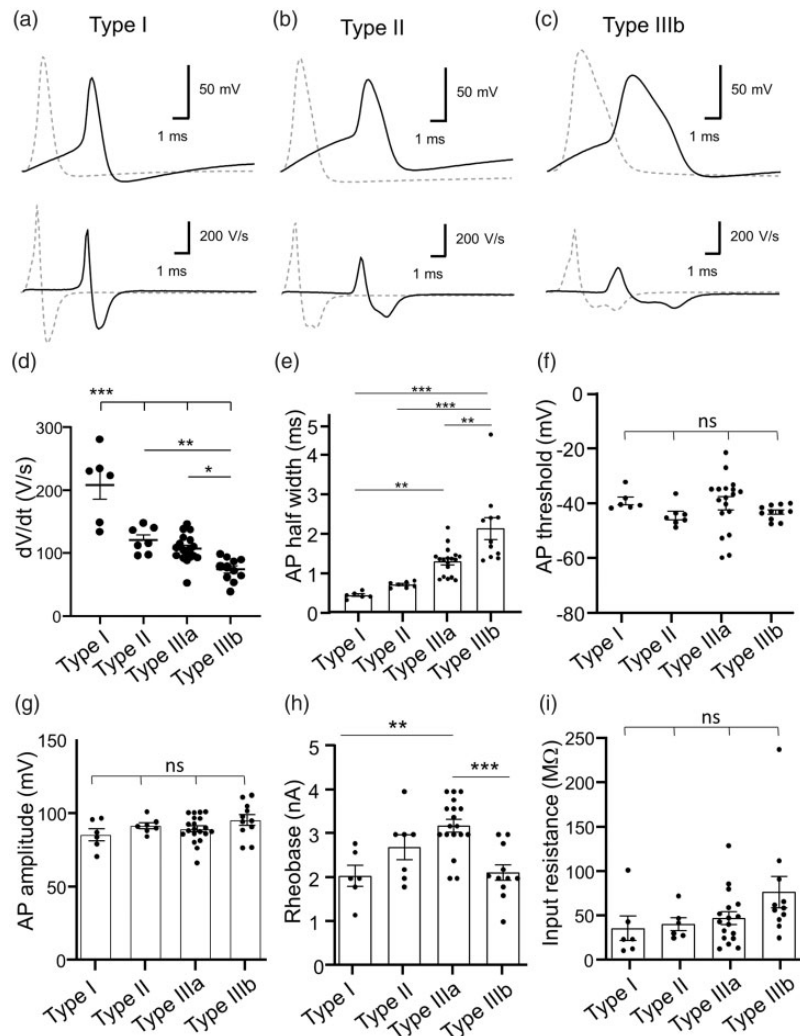


Figure 5. Properties of action potentials elicited by direct current injections into the somas of V2 A β -afferent neurons. Three sets of sample traces (solid dark) show APs (top) and their derivatives with time (dV/dt, bottom) in a type I (a), a type II (b) and a type IIIb (c) V2 trigeminal A β -afferent neurons following current injections into the somas of the recorded neurons. The gray dashed traces are APs (top) elicited by peripheral electrical stimulation (top panels) and their dV/dt (bottom). (d) The dV/dt values of negative peaks of repolarization for type I (n = 6), type II (n = 7), type IIIa (n = 18), and type IIIb (n = 11) V2 trigeminal A β -afferent neurons. Summary data of AP half widths (e), AP threshold (f), AP amplitude (g), AP rheobase (h), and input resistance (i) of the four types of V2 trigeminal A β -afferent neurons. Each symbol represents an individual experimental observation, mean \pm SEM is also shown; ns, no significant difference; *P < 0.05, **P < 0.001, *** P < 0.001.

were voltage-activated K⁺ currents. While there were no obvious differences in the kinetics of the outward currents among the four types of V2 trigeminal A β -afferent neurons (Figure 6(a)), the amplitudes of the outward currents were found to be relatively smaller in type IIIb V2 trigeminal A β -afferent neurons in comparison with type I and type IIIa V2 trigeminal A β -afferent neurons (Figure 6(b)).

Discussion

In the present study, we have characterized V2 trigeminal A β -afferent neurons and classified them into four

subtypes based on their AP properties. We show that a number of AP parameters are significantly different among V2 trigeminal A β -afferent neurons. These parameters include the dV/dt of AP repolarization, AP conduction velocities, AP widths, AHP durations, and AP conduction success rates in response to high frequency stimulation. These AP parameters may be useful electrophysiological indicators of functional subtypes of V2 trigeminal A β -afferents such as non-nociceptive-like and nociceptive-like V2 trigeminal A β -afferents. The classification of V2 trigeminal A β -afferent neurons may help future studies on the roles of V2 trigeminal A β -afferents in different sensory functions and their potential

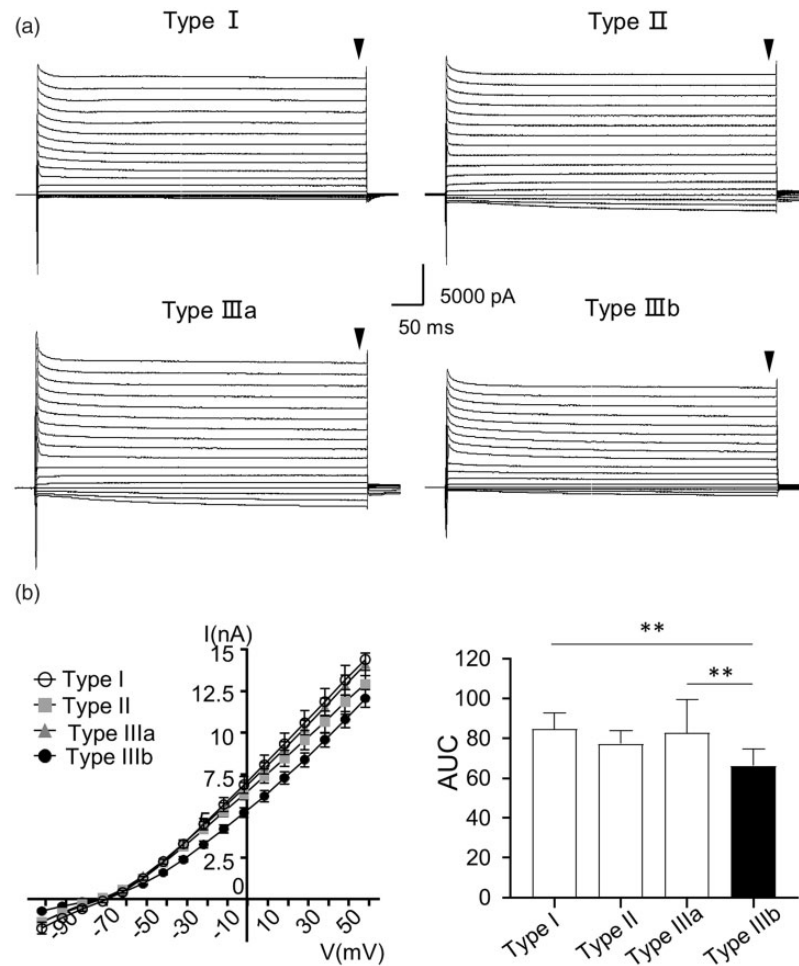


Figure 6. Voltage-activated outward currents in different types of V2 A β -afferents. (a) Four sets of sample traces of voltage-activated currents recorded from type I (top left), type II (top right), type IIIa (bottom left), and type IIIb (bottom right) V2 trigeminal A β -afferent neurons. Arrowhead in each panel indicates the place where currents were measured and plotted in (b). (b) Left, I-V curves of currents measured at the arrowhead-indicated places in A for type I (n = 6), type II, (n = 7), type IIIa (n = 18) and type IIIb (n = 11) V2 trigeminal A β -afferent neurons. Right, area under the I-V curves (AUC) of the left panel for statistical comparison of the outward currents in type I (n = 6), type II, (n = 7), type IIIa (n = 18), and type IIIb (n = 11) V2 trigeminal A β -afferent neurons. Data represent mean \pm SEM; **P < 0.001.

involvement in pain such as mechanical allodynia under pathological conditions.

Previous *in vitro* studies on electrophysiological properties of somatosensory neurons were mostly performed with DRG neurons or TG neurons dissociated from their ganglions.^{15,16} Most of previous electrophysiological studies were performed on small-sized somatosensory neurons.^{15,16} Since large-sized somatosensory neurons usually do not survive in cell dissociation procedures, electrophysiological properties of large-sized neurons (i.e. A β -afferent neurons) were not well characterized previously. In the present study, *ex vivo* TG preparations were used and large-sized V2 trigeminal afferent neurons were healthy in our TG preparations. This allowed us to apply patch-clamp recordings to characterize electrophysiological properties of V2 trigeminal A β -afferent neurons.

We have considered V2 trigeminal afferents with conduction velocities more than 10 m/s as A β -afferents in the present study. Most V2 trigeminal afferents in the present study had conduction velocities higher than 10 m/s. Previous studies have considered conduction velocity of 10 m/s as the border between A δ - and A β -afferent fibers in rats.⁴ However, a previous study in rat trigeminal afferent nerves defined A β -afferent fibers as those with conduction velocities more than 14 m/s.¹⁷ It should be noted that our experiments were performed at the room temperature of 24 °C while previous studies were mostly performed at temperatures between 30 °C to 37 °C.^{4,17} It has been shown in rat sciatic nerves that the conduction velocity varied about 1.2 m/s per degree centigrade over the range of 20–40 °C.¹⁸ Therefore, all our A β fibers would have conduction

velocities well above 14 m/s if our experiments were conducted at temperatures higher than 30 °C. In addition to conduction velocity, other membrane and action potential parameters reported in our study may also differ to some extent from those determined at higher temperatures in previous studies. We performed our *in vitro* patch-clamp recording experiments at the room temperature of 24 °C rather than at higher temperatures between 30 °C to 37 °C because TG neurons could be kept healthy for longer time at the room temperature of 24 °C during our *in vitro* experiments. In DRG neurons, large-sized neurons were defined as those with soma mean diameters of $\geq 45 \mu\text{m}$, and the large-sized DRG neurons were usually A β -afferents. In our V2 trigeminal afferent neurons, in addition to those cells with mean diameters $\geq 45 \mu\text{m}$, cells with mean diameters in the range of 40 to 45 μm were also found to be A β -afferents based on the conduction velocity measured in the present study. Since V2 TGs do not contain proprioceptive A α -afferents, it is a strength of using V2 TGs for determining the properties of A β -afferents without unintended inclusion of A α -afferents.

We show in the present study that among the four types of V2 trigeminal A β -afferent neurons the type I neurons have the largest dV/dt of AP repolarization, the shortest AP widths and AHP80 durations, and the highest AP success rates. In contrast, type IIIb V2 trigeminal A β -afferent neurons have the smallest dV/dt of repolarization, the longest AP widths and AHP80 durations, and the lowest AP success rates. These discrete AP properties were observed regardless of APs elicited by electrical stimulation at the peripheral endings or at the soma of V2 trigeminal A β -afferent neurons. While we can classify V2 trigeminal A β -afferent neurons into 4 subtypes based on AP parameters, we have not directly determined whether these subtypes of V2 trigeminal A β -afferent neurons are functionally distinct groups of somatosensory neurons. Previous *in vivo* recordings from the somas of DRG neurons have shown that different functional groups of A β -afferent neurons display distinguished AP properties.^{4,7} For example, previous *in vivo* recordings have shown that LTMR A β -afferent neurons in DRGs have APs with rapid kinetics, large dV/dt without inflection in repolarization phase, short AP widths and AHP durations.^{4,6,11} In our study, the type I V2 trigeminal A β -afferent neurons have the AP properties similar to those of LTMR A β -afferent DRG neurons shown in the previous studies.^{4,6,11} However, the numbers of type I neurons were relatively small in the present study, which could be due to a biased sampling of neurons in our recordings. Previous studies also have shown that nociceptive A β -afferent neurons in DRGs have APs with slow kinetics, small dV/dt with inflection in repolarization, and longer action potential widths and AHP durations.^{4,6,11} Nociceptive A β -afferent

neurons have been found to account for approximately 20% of A β -afferent neurons in DRGs of rats.^{4,7} In the present study, we have found that the majority of V2 trigeminal A β -afferent neurons, except type I neurons, have APs with slower kinetics, smaller dV/dt with inflection, and longer action potential widths, and longer AHP durations. It is less likely that all V2 trigeminal A β -afferent neurons in type II, type IIIa, and type IIIb groups were nociceptive A β -afferent neurons. These three types of neurons may include both non-nociceptive and nociceptive V2 trigeminal A β -afferents. Previous studies in DRG neurons have observed two subtypes of A β -afferent nociceptive neurons, the HTMR (high threshold mechanoreceptors) and the unresponsive A β -afferent nociceptive neurons.¹⁹ The HTMR A β -afferent nociceptive neurons were shown to have relatively faster AP kinetic while the unresponsive A β -afferent nociceptors have very slow AP kinetics.¹⁹ In our V2 trigeminal A β -afferent neurons, we have shown that type II V2 trigeminal A β -afferent neurons have relatively faster APs similar to those of HTMR DRG neurons identified in the previous studies.¹⁹ On the other hand, type IIIb V2 trigeminal A β -afferent neurons had the slowest AP kinetics similar to those of unresponsive nociceptive A β -afferent DRG neurons shown in previous studies.¹⁹ In the present study, we show that AP success rates in response to high frequency stimulation are significantly different among the 4 different types of V2 trigeminal A β -afferents. To our knowledge, this electrophysiological property of A β -afferents has not been characterized in previous studies. We have found that type I V2 trigeminal A β -afferents had the highest and type IIIb V2 trigeminal A β -afferents had the lowest AP conduction success rates. The responses to high frequency stimulation may be another useful electrophysiological indicator for different functional types of A β -afferents. In the present study, we also examined voltage-activated currents in the four types of V2 trigeminal A β -afferents. We have found that type IIIb V2 trigeminal A β -afferent neurons have relatively smaller voltage-activated K⁺ outward currents in comparison with the other types of V2 trigeminal A β -afferent neurons. This may be a factor causing the slower AP repolarization in type IIIb V2 trigeminal A β -afferent neurons. More detailed studies on voltage-activated currents in V2 trigeminal A β -afferent neurons need to be performed to provide ion channel mechanisms underlying the distinguished AP properties of different types of V2 trigeminal A β -afferent neurons.

In addition to their roles in both low threshold and high threshold mechanical responses, A β -afferent fibers have been suggested to play a key role in mechanical allodynia and spontaneous pain under pathological conditions including tissue inflammation and neuropathy.^{8,19–22} Furthermore, a previous study using a

pharmacological approach to silence A β -afferent fibers has shown the alleviation of neuropathic pain in animal models.²³ Our characterizations of V2 trigeminal A β -afferent fibers may help us in future to explore sensory functions of different types of V2 trigeminal A β -afferent fibers in orofacial regions under both physiological and pathological conditions.

Author Contributions

JGG conceived and designed the experiments and wrote the paper. YO performed electrophysiology experiments and data analysis. AY, ST and RJV provided technical assistance, and participated in data analysis and discussion.

Declaration of Conflicting Interests

The author(s) declared no potential conflicts of interest with respect to the research, authorship, and/or publication of this article.

Funding

The author(s) disclosed receipt of the following financial support for the research, authorship, and/or publication of this article: This study was supported by NIH grants DE018661 and DE023090 to J.G.G.

ORCID iD

Jianguo G Gu  <https://orcid.org/0000-0002-8404-9850>

References

1. Light AR. Peripheral sensory systems. In: Dyck PJ, Griffin JW, Low PA, et al. (eds) *Peripheral neuropathy*. Philadelphia: W. B. Saunders, 1993, pp. 149–165.
2. Vermeiren S, Bellefroid EJ, Desiderio S. Vertebrate sensory ganglia: common and divergent features of the transcriptional programs generating their functional specialization. *Front Cell Dev Biol* 2020; 8: 587699.
3. Li L, Rutlin M, Abaira VE, Cassidy C, Kus L, Gong S, Jankowski MP, Luo W, Heintz N, Koerber HR, Woodbury CJ, Ginty DD. The functional organization of cutaneous low-threshold mechanosensory neurons. *Cell* 2011; 147: 1615–1627.
4. Djouhri L, Lawson SN. Abeta-fiber nociceptive primary afferent neurons: a review of incidence and properties in relation to other afferent A-fiber neurons in mammals. *Brain Res Brain Res Rev* 2004; 46: 131–145.
5. Fang X, McMullan S, Lawson SN, Djouhri L. Electrophysiological differences between nociceptive and non-nociceptive dorsal root ganglion neurones in the rat in vivo. *J Physiol* 2005; 565: 927–943.
6. Koerber HR, Druzinsky RE, Mendell LM. Properties of somata of spinal dorsal root ganglion cells differ according to peripheral receptor innervated. *J Neurophysiol* 1988; 60: 1584–1596.
7. Lawson SN, Fang X, Djouhri L. Nociceptor subtypes and their incidence in rat lumbar dorsal root ganglia (DRGs): focussing on C-polymodal nociceptors, abeta-nociceptors, moderate pressure receptors and their receptive field depths. *Curr Opin Physiol* 2019; 11: 125–146.
8. Djouhri L. L5 spinal nerve axotomy induces sensitization of cutaneous L4 abeta-nociceptive dorsal root ganglion neurons in the rat in vivo. *Neurosci Lett* 2016; 624: 72–77.
9. Tashima R, Koga K, Sekine M, Kanehisa K, Kohro Y, Tominaga K, Matsushita K, Tozaki-Saitoh H, Fukazawa Y, Inoue K, Yawo H, Furue H, Tsuda M. Optogenetic activation of non-nociceptive abeta fibers induces neuropathic pain-like sensory and emotional behaviors after nerve injury in rats. *eNeuro* 2018; 5: ENEURO.0450-17.2018.
10. Ritter AM, Mendell LM. Somal membrane properties of physiologically identified sensory neurons in the rat: effects of nerve growth factor. *J Neurophysiol* 1992; 68: 2033–2041.
11. Rose RD, Koerber HR, Sedivec MJ, Mendell LM. Somal action potential duration differs in identified primary afferents. *Neurosci Lett* 1986; 63: 259–264.
12. Kanda H, Ling J, Chang YT, Erol F, Viatchenko-Karpinski V, Yamada A, Noguchi K, Gu JG. Kv4.3 channel dysfunction contributes to trigeminal neuropathic pain manifested with orofacial cold hypersensitivity in rats. *J Neurosci* 2021; 41: 2091–2105.
13. Ling J, Erol F, Viatchenko-Karpinski V, Kanda H, Gu JG. Orofacial neuropathic pain induced by oxaliplatin: down-regulation of KCNQ2 channels in V2 trigeminal ganglion neurons and treatment by the KCNQ2 channel potentiator retigabine. *Mol Pain* 2017; 13: 1744806917724715.
14. Viatchenko-Karpinski V, Erol F, Ling J, Reed W, Gu JG. Orofacial operant behaviors and electrophysiological properties of trigeminal ganglion neurons following masseter muscle inflammation in rats. *Neurosci Lett* 2019; 694: 208–214.
15. Viatchenko-Karpinski V, Ling J, Gu JG. Down-regulation of Kv4.3 channels and a-type K(+) currents in V2 trigeminal ganglion neurons of rats following oxaliplatin treatment. *Mol Pain* 2018; 14: 1744806917750995.
16. Viatchenko-Karpinski V, Gu JG. Mechanical sensitivity and electrophysiological properties of acutely dissociated dorsal root ganglion neurons of rats. *Neurosci Lett* 2016; 634: 70–75.
17. Kitagawa J, Takeda M, Suzuki I, Kadoi J, Tsuboi Y, Honda K, Matsumoto S, Nakagawa H, Tanabe A, Iwata K. Mechanisms involved in modulation of trigeminal primary afferent activity in rats with peripheral mononeuropathy. *Eur J Neurosci* 2006; 24: 1976–1986.
18. Birren JE, Wall PD. Age changes in conduction velocity, refractory period, number of fibers, connective tissue space and blood vessels in sciatic nerve of rats. *J Comp Neurol* 1956; 104: 1–16.
19. Wu Q, Henry JL. Delayed onset of changes in soma action potential genesis in nociceptive A-beta DRG

- neurons in vivo in a rat model of osteoarthritis. *Mol Pain* 2009; 5: 57.
20. Devor M. Ectopic discharge in abeta afferents as a source of neuropathic pain. *Exp Brain Res* 2009; 196: 115–128.
 21. Wu Q, Henry JL. Changes in abeta non-nociceptive primary sensory neurons in a rat model of osteoarthritis pain. *Mol Pain* 2010; 6: 37.
 22. Zhu YF, Henry JL. Excitability of abeta sensory neurons is altered in an animal model of peripheral neuropathy. *BMC Neurosci* 2012; 13: 15.
 23. Xu ZZ, Kim YH, Bang S, Zhang Y, Berta T, Wang F, Oh SB, Ji RR. Inhibition of mechanical allodynia in neuropathic pain by TLR5-mediated A-fiber blockade. *Nat Med* 2015; 21: 1326–1331.